Available online at www.sciencedirect.com
ScienceDirect
Journal of the European Ceramic Society 27 (2007) 2597–2603
www.elsevier.com/locate/jeurceramsoc

Fracture test of thin sheet electrolytes for solid oxide fuel cells

Jürgen Malzbender*, Rolf W. Steinbrech

Forschungszentrum Jülich GmbH, Institute of Energy Research (IEF-2), 52425 Juelich, Germany

Received 11 August 2006; received in revised form 2 November 2006; accepted 10 November 2006
Available online 26 December 2006

Abstract

The fracture stress of the electrolyte determines the limit of the mechanical integrity of electrolyte supported solid oxide fuel cells. However, the measurement of the fracture stress of thin sheet specimens typically leads to difficulties in experiment and analysis. In particular evaluation problems arise in bending tests due to the non-linear deformation behaviour. In addition to conventional bi-axial bending tests of 6ScSZ and 3YSZ electrolyte foils with a thickness of ~100 μm a new method is introduced, which relies on ring-on-ring tests with composite specimens. By gluing the thin electrolyte foil on a steel substrate, non-linear deformation of the foils is avoided. The method allows the correlation of the fracture stress with a defined electrolyte portion under maximum stress and hence a prediction of failure stresses and probabilities for real-size cells. The results reveal a higher characteristic fracture stress and Weibull modulus for the 3YSZ foils compared to those of the 6ScSZ variant. In both electrolyte materials, failure of the foils appeared to be related to surface defects.

Keywords: Solid oxide fuel cells; Fracture; Strength; Failure analysis; Tape casting

1. Introduction

Planar solid oxide fuel cells (SOFCs) are currently being developed in two main geometrical variants with different structural support. SOFC concepts based on electrode substrates (mostly anode) allow a reduction of the electrolyte thickness to thin layers of 5–10 μm.[1] In contrast, in the electrolyte supported variant a much thicker membrane (~100–200 μm) is required for mechanical robustness. Since the cell resistance strongly depends on electrolyte thickness, the electrode supported SOFC concept has the attractive advantage of lower operation temperature at equal electrochemical performance.

The differences in the thermo-elastic behaviour between the individual layers in the planar SOFC cell composite generate residual stresses[2,3] that can cause mechanical integrity problems. In the case of an anode supported cell design, compressive stresses exist in the thin film electrolyte, which usually has the smaller thermal expansion. Accordingly the anode will exhibit tensile stresses. In an electrolyte supported design, the electrolyte will be under a lower compressive stress, whereas the tensile stress in the anode is enhanced.

However, there are some specific advantages of the electrolyte supported cell concept with respect to mechanical integrity. The asymmetric variant with the electrode support typically exhibits, if unconstrained, considerable cell curvature.[4] The electrolyte supported cell has a more or less symmetric layer structure and thus the residual stresses generate less curvature, i.e. the cells are essentially flat. Also the impact of anode re-oxidation strain on cell failure, a phenomenon well known for anode supported SOFCs,[5] is considered to be less severe when the electrolyte, which is thicker and denser than the porous anode dominates the mechanical behaviour. Of course ultimately all assembly, operation and residual stresses have to remain below the strength of a material.

Electrolyte materials with high conductivity and high fracture stress in thin sheet geometry appear to be attractive for further promoting the electrolyte supported SOFC concept. Thus from the electrochemical point of view, the substitution of the currently standard yttria-stabilised zirconia (YSZ) electrolyte by a scandia-stabilised zirconia with higher conductivity is one of the material options.[6] However, there are few data available on the mechanical properties of thin sheet material. Although some

* Corresponding author. Tel.: +49 2461 616964; fax: +49 2561 613699.
E-mail address: j.malzbender@fz-juelich.de (J. Malzbender).

0955-2219/$ – see front matter © 2006 Elsevier Ltd. All rights reserved.
doi:10.1016/j.jeurceramsoc.2006.11.071

studies of the mechanical properties of SOFC materials exist,[7,8] a comparison of the fracture strength of thin sheet ScSZ and YSZ electrolytes is lacking. Moreover, the accurate measurement of the fracture stress of thin electrolyte foils is still a difficult task in itself.[9]

The present work focuses on the fracture stress characterisation of ~100 μm thick 6ScSZ and 3YSZ foils based on a new testing methodology for thin foils. Among the different mechanical testing methods for thin sheet specimens, the ring-on-ring bending has been selected. Measurements have been carried out with free-standing foils at room temperature (RT) and 800 °C and in a novel approach at RT with foils glued to a metallic substrate. Also the effect of the different surfaces morphologies specific for tape cast electrolyte foils is examined. The obtained characteristic fracture stresses are correlated with the stressed specimen surface area using Weibull statistics. Therefore also fracture data could be derived which are relevant for larger cells typically used in SOFC stacks.

2. Testing methods and alternative specimen design

The fracture stress values of ceramic specimens typically show a considerable scatter due to the defect/flaw size distribution. This scatter can be assessed statistically using the characteristic fracture stress (modulus of rupture, MOR) and the Weibull modulus.[10] Based on the reasonable assumption that the flaw distribution does not depend on the specimen size, these two statistical parameters permit a calculation of the fracture stress for different specimen and component sizes. The MOR decreases with increasing specimen size as a result of the increased probability of detecting large defects. Depending on the defect type, the MOR scales either with surface area or volume under maximum tensile stress. Hence the characteristic fracture stress is a specific value for a discrete specimen size. Therefore a calculation of the failure probability of an electrolyte in a SOFC stack requires consideration of the ratio of respective cell size to tested specimen size.

The ring-on-ring test (co-axial ring or double ring test) is conveniently used for bending plate-like brittle specimens. An important advantage of the method is that defects, which might be induced by specimen shaping, e.g. cutting edges, do not influence the measured fracture stress. However, linear bending theory is only valid if the deflection of the specimen does not exceed a discrete value. The critical deflection depends on the ratio of the loading to supporting ring and is ~50% of the specimen thickness for a ratio of two.[11–13] At such large deflections the specimen stress has a localized maximum above the loading ring, contrary to the small deflection situation with a constant tensile stress within the specimen portion defined by the loading ring. Thus fracture of thin sheet electrolyte specimens will occur preferentially above the loading ring. In the large deflection case,[14] finite element analysis can be used to determine the fracture stress of the electrolyte material. However, the specific volume or area above the loading ring, which exhibited the maximum tensile stress remains as an unknown parameter.

Membrane tests, where vacuum or pressure rather than a mechanical load is applied for deflecting the specimen, generate in principle a similar stress concentration pattern, but the non-linearity effect can be reduced by appropriate design of the testing facility. However, fixation of the specimen and their sealing can lead to local changes in curvature and hence stress maxima.[15]

In principle non-linear behaviour is avoided in pure tensile tests. The fracture stresses can be affected by specimen preparation and the mechanical gripping of the thin sheet specimens. In particular, a flawless preparation of thin specimen edges is very difficult.[9] Alternatively, tensile stresses can also be induced by fixation of a thin sheet specimen to a material with different thermal expansion coefficient and subsequent heating or cooling. However, depending on the fracture stress and thermal expansion coefficients of the involved materials, a difference of a few 100 K might be necessary to cause fracture. Furthermore, due to the statistical distribution of defects each specimen will fail at a different temperature and hence the characteristic fracture stresses cannot be associated with one particular temperature.

The problems associated with the determination of the fracture stress of thin sheet specimens led to the development of an alternative testing method. Composite specimens were prepared for ring-on-ring bending tests. Essentially the thin electrolyte sheet was glued onto the surface of thicker steel substrates and loaded so that the electrolyte was only under tensile bending. The additional substrate led to a larger total specimen thickness and reduced the stress localisation. Since the composite deflection at fracture was less than half the total thickness, no local stress maxima occurred in the electrolyte. The ring-on-ring test with the composite specimens permitted a determination of the specimen portion under maximum stress. The stressed surface area of free-standing electrolyte specimens could then be estimated, a value not assessable from finite element based analysis of large deflection experiments.[14]

3. Experimental

Thin sheet electrolyte material of 6ScSZ (6 wt.% Scandia Stabilized Zirconia, Nippon Shokubai) and 3YSZ (3 wt.% Yttria Stabilized Zirconia, Indec) was analysed. The thickness of the 50 mm × 50 mm sheets was ~110 μm for the 6ScSZ and ~100 μm for the 3YSZ. The foils were laser cut into smaller specimens of 24 mm × 24 mm. Some of the specimens were tested as cut, and some were glued to an Alloy 617 substrate to obtain a composite specimen. The Alloy 617 substrates had a thickness of 550 and 650 μm. A commercially available fast hardening adhesive (Pattex-Cyanoacrylat) was used to glue the electrolyte foils to the substrates. The gluing method did not involve a high-temperature cure, which might result in residual stress. The free-standing specimens were tested at room temperature (RT) and 800 °C, the composite specimens only at RT.

All mechanical tests were carried out in ring-on-ring loading using an electro-mechanical universal testing machine (INSTRON 1362) with digital fast track control. The supporting ring had a radius of ~10 mm, the loading ring a radius of ~5 mm.

The experiments were performed in load control mode with a constant rate of 50 N/min. The elastic moduli of the 6ScSZ and 3YSZ foils were determined by depth sensing indentation (Fischerscope 100),[16] yielding a common average value of 195 GPa for both materials.

4. Theory

The specimen stress in a ring-on-ring test with isotropic material can be calculated, as long as the deflection is less than half the specimen thickness, using[13]:

$$\sigma = \frac{3(1+\mu)}{2\pi}\left[\ln\frac{r_2}{r_1} + \frac{1-\mu}{1+\mu}\times\frac{r_2^2 - r_1^2}{2r_3^2}\right]\frac{F}{t^2} \quad (1)$$

where F is the applied force, t is the specimen thickness, and r_1, r_2 and r_3 are the radii of the load ring, supporting ring and (circular) specimen, respectively. Eq. (1) also contains the Poisson ratio μ. In the case of square specimens with the side length L an equivalent average radius r_{3m} has to be substituted for r_3, which can be estimated using[11,13]:

$$r_{3m} = \frac{1+\sqrt{2}}{2}\times\frac{L}{2} \approx 0.60\,L \quad (2)$$

For large deflections the non-linearity problem can be circumvented in part using calibration curves given in the literature.[12,17] Based on these literature results, an analytical approximation relation, which explicitly considers the ratio of deflection to specimen thickness (d/t), can be proposed:

$$\sigma = E\left(0.1216\left(\frac{d}{t}\right)^3 + 0.1643\left(\frac{d}{t}\right)^2 + 1.6987\left(\frac{d}{t}\right) + 0.02378\right)\frac{t^2}{r_2^2} \quad (3)$$

In the case of a layered composite, such as the proposed chosen present geometry of the electrolyte foil glued on a substrate, the stress in the surface of the electrolyte foil is[10]:

$$\sigma_{f,E} = \frac{FE_E}{4\pi(1-\nu_n{}^2)D^*}(t_{ges} - t_n) \times\left[(1+\nu)\ln\left(\frac{r_2}{r_1}\right) + \frac{1-\nu}{2}\left(\frac{r_2^2 - r_1^2}{r_3^2}\right)\right] \quad (4)$$

In Eq. (4) the stiffness $D = Et^3/12\,(1-\nu^2)$ of an isotropic material was substituted by the composite stiffness D^*. For a n-layered composite D^* is[10]:

$$(D)^* = \frac{1}{3}\sum_{i=1}^{n}\frac{E_i}{1-\nu_i^2}\left(\left(\sum_{j=1}^{i}t_j - t_n\right)^3 + \left(t_n - \sum_{j=1}^{i-1}t_j\right)^3\right) \quad (5)$$

In addition the position of the neutral axis changes in the composite to:

$$t_n = \sum_{i=1}^{n}\frac{E_i}{1-\nu_i^2}w_i t_i \frac{\left(2\sum_{j=1}^{i-1}t_j + t_i\right)}{\left(2\sum_{i=1}^{n}(E_i/1-\nu_i^2)w_i t_i\right)} \quad (6)$$

The composite specimens consisted of materials 1–3, the electrolyte foil, glue and substrate. The elastic moduli were measured using indentation testing. Thicknesses were measured before and after the gluing. The elastic modulus of the glue had a minor influence on the determination due to its small thickness and close distance to the neutral bending axis.

The fracture stresses values derived from Eqs. (3) and (4) were used for a statistical Weibull analysis based on DIN 51110-3 (identical to DIN ENV 843-5):

$$P_f = 1 - \exp\left[-\left(\frac{\sigma}{\sigma_0}\right)^m\right] \quad (7)$$

with the characteristic strength σ_0 and the Weibull parameter m. P_f is the failure probability.

5. Results and discussion

First the fracture stress results of the 6ScSZ and 3YSZ electrolyte foils are discussed separately, and then a comparison of the values for the two electrolyte foil materials is made.

5.1. 6ScSZ electrolyte foils

The tape cast 6ScSZ electrolyte foils possessed surfaces of different roughness and morphology (Fig. 1). Hence, in order to test possible surface effects, two specimens sets, one with the rougher, the other with the smoother surface under tension, were tested at RT. Typical load–deflection curves obtained using ring-on-ring tests at RT for free-standing 6ScSZ foils with the rougher surface under tension are shown in Fig. 2. The general shape of the curves matches well, but there is considerable scatter in the fracture loads. In many cases a deflection of approximately three times the sheet thickness (~300 μm) was reached at specimen failure.

Using the approximation in Eq. (3) and the Weibull statistics of Eq. (7), values of $\sigma_0 = 780 \pm 40$ MPa and $m = 5 \pm 2$ were obtained. Curves of similar shape were also measured for the specimens with the smoother surface under tension. However, the statistical data evaluation leads to $\sigma_0 = 1080 \pm 40$ MPa and $m = 8 \pm 3$, proving the mechanically superior properties behavior of the smoother surface.

The dependence of strength on the surface roughness also indicates that the failure of the foils is governed by surface properties rather than by volume defects. This information about the fracture origin will become important below. Further testing concentrated on the rougher surface, since it has been shown to be mechanically inferior.

Load - deflection curves of similar shape as in Fig. 2 were obtained for free-standing foils at 800 °C with the rougher surface in tension, but failure occurred at lower deflections (range of 1.5–1.9 times the thickness). Also the average fracture load

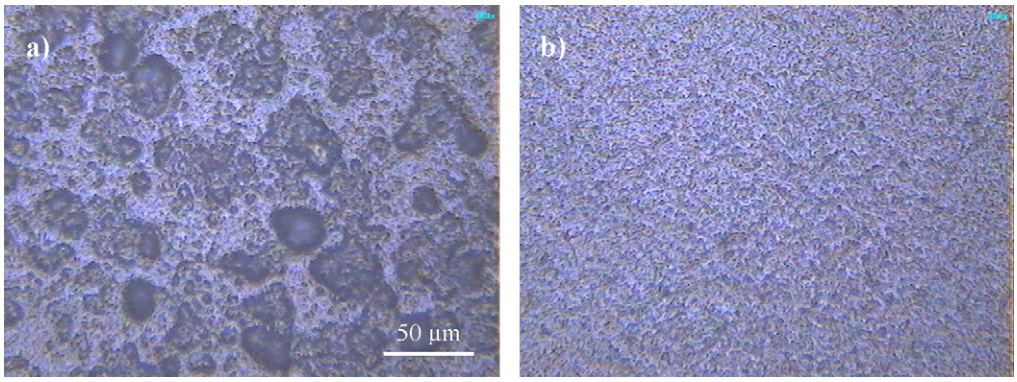

Fig. 1. Typical surface morphologies of the tested 6ScSZ electrolyte foils. (a) Rougher surface and (b) smoother surface.

was by a factor of ∼2.4 smaller than the value obtained at RT. In general, at 800 °C the load at a discrete deflection was about 10% lower than at RT, implying a ∼10% lower stiffness. Again, the experimental data can be evaluated using the approximation in Eq. (3). The resulting characteristic fracture stress is $\sigma_0 = 430 \pm 21$ MPa with a Weibull modulus of $m = 6 \pm 2$. The Weibull modulus agrees within the limits of uncertainty with the value obtained at RT, whereas, the characteristic fracture stress is lower by a factor of ∼1.8.

Load–deflection curves for the composite specimens with the 6ScSZ electrolyte foils glued to Alloy 617 substrate are shown in Fig. 3. The curves are essentially linear and predominantly governed by the mechanical behavior of the substrate. The two different slopes in Fig. 3 reflect the two different substrate thicknesses of 550 and 650 µm used in the tests, respectively. The slope of the curves is in agreement with prediction based on Eq. (5). Although the substrate dominates the deformation of the composite specimens, the fracture of the 6ScSZ electrolyte foil can be clearly recognized as a kink in the curves. The associated loads yield a characteristic fracture stress of $\sigma_0 = 230 \pm 14$ MPa ($m = 4.1 \pm 1.2$).

A summarizing Weibull plot of the data for the 6ScSZ foils from the three sets of experiments is shown in Fig. 4. Since the m values agree within the limits of uncertainty for the free-standing and glued electrolytes, further statistical considerations of the relationship between characteristic fracture stress and stressed specimen size can be made.

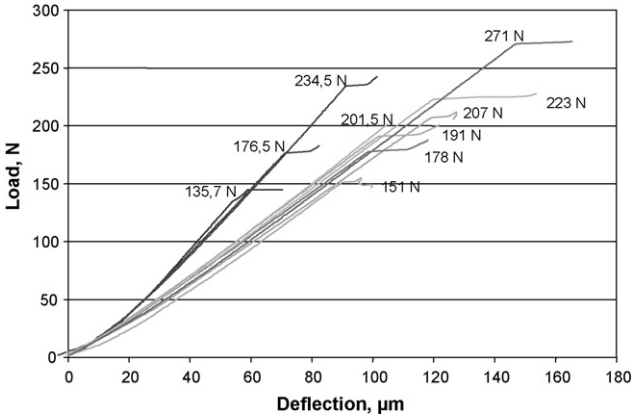

Fig. 3. Load deflection curves of 6ScSZ foils glued on metallic substrate.

In general the number of measurements performed in the present study is too low to obtain an accurate Weibull modulus. To obtain a higher accuracy for further evaluation of the present data, we assume that all sets of the sheet specimens possess the same Weibull modulus. This assumption appears to be reasonable, since all specimens were cut from plates of the same 6ScSZ batch. Hence the fracture stresses of each set were normalized by the individual characteristic fracture stress. The normalized data of all sets were then treated together. Thus for the tested 27 specimens a single Weibull modulus characteristic for the 6ScSZ foils of $m = 5.3 \pm 1.0$ is obtained.

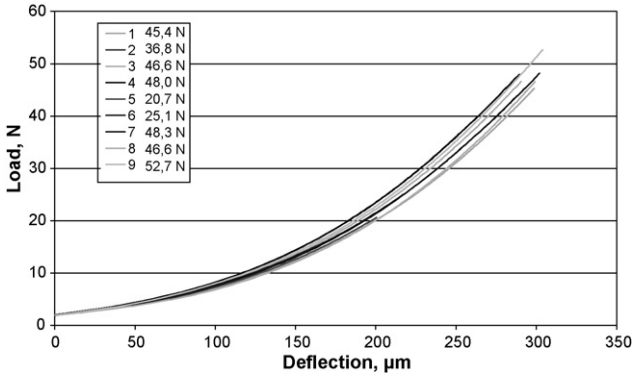

Fig. 2. Load deflection curves of free standing 6ScSZ electrolyte specimens with the rougher surface under tension.

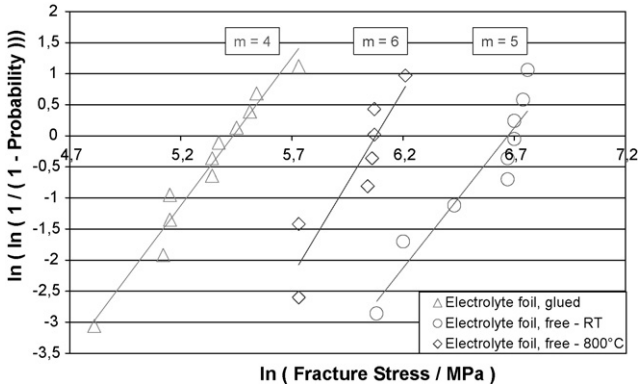

Fig. 4. Weibull plot of the fracture stresses for glued and free 6ScSZ electrolyte foils.

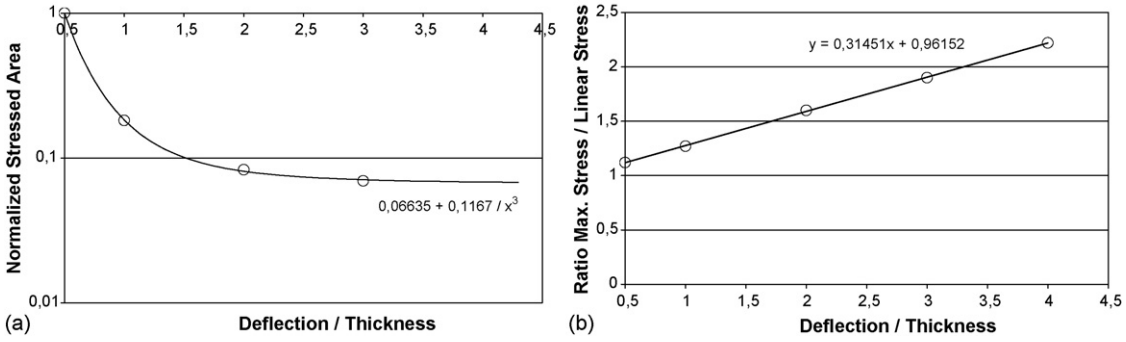

Fig. 5. Results from FEM simulation. (a) Normalized surface area experiencing 90% of the maximum stress. (b) Normalized stress. (Parameter in the simulation: $t = 100\,\mu m$, $r_1 = 4.5\,mm$, $r_2 = 2\,r_1$, $E = 200\,GPa$).

The above results imply that the fractures may be associated with surface defects. The relationship between the characteristic fracture stresses $\sigma_{0,A1}$ and $\sigma_{0,A2}$ of the stressed surface areas A_1 and A_2 of the two testing geometries can be estimated by:

$$\frac{\sigma_{0,A1}}{\sigma_{0,A2}} = \left(\frac{A_1}{A_2}\right)^{-1/m} \tag{8}$$

Eq. (8) can be used to estimate the stressed area in the ring-on-ring tests of free-standing foils based on the results for glued 6ScSZ composite specimens. Note that the use of Eq. (8) is only an approximation since it assumes that the stress distributions are equivalent and in a more severe calculation stress-area integrals should be used.

The surface area under tension in the tests with glued foils was $78.5\,mm^2$ (area within the loading ring). Using the average Weibull modulus of $m = 5.3$, the stressed surface area of the free-standing electrolyte foil is calculated from Eq. (8) as $\sim 0.12\,mm^2$. The expected maximum stress at the location of the loading ring suggests that the stressed surface area correlates with the diameter of the loading ring ($\sim 10\,mm$) yielding a width of the stressed concentric surface area of $\sim 0.01\,mm$.

As a first approximation this value might also be used for the stressed surface area at high temperature. However, the free-standing electrolyte foils tested at high temperatures fractured at a lower ratio of deflection to thickness; hence the stressed surface area was also larger. Using the radial stress profiles presented in[12] and assuming that the width of the stressed surface area can be associated with 90% of the maximum stress, a $\sim 20\%$ increase can be expected, which changes the ratio in Eq. (8) by only $\sim 3.5\%$.

This was verified using finite element simulation using the finite element code ANSYS for the particular experimental parameters in this study. As shown in Fig. 5a) the decrease in width of the stressed area is small at large deflections and agrees quite well with the 20% estimated above. In addition Fig. 5b) shows the normalized stress (stress above the loading ring divided by the stress as calculated using linear theory), which is linearly proportional to the deflection/thickness ratio.

Based on these geometrical considerations, the experimentally determined characteristic fracture stresses are plotted in Fig. 6 as a function of stressed surface area together with the theoretical curves of Eq. (8). The characteristic fracture stress of larger electrolyte sheets used in a SOFC stack can now be predicted. The characteristic strength of a $10\,cm \times 10\,cm$ cell of the 6ScSZ electrolyte material should be 90 ± 40 and $50 \pm 20\,MPa$ at RT and 800 °C, respectively. A further reduction of the maximum applicable stress on 6ScSZ electrolytes needs to be taken into account for lower failure probability (see Eq. (7)). If the failure of only one cell in 1000 is permitted stress limits of 25^{+20}_{-14} and $14^{+11}_{-8}\,MPa$ at RT and 800 °C respectively, should not be exceeded.

The calculation of the characteristic strength of larger cells at RT is exclusively based on the results of the glued foils since the estimated area for the free electrolyte foils is derived from the measurements of the glued foils. Hence, an increase in the characteristic strength of the free foils by a factor of n, which might be a result of an uncertainty in Eq. (3), would not affect the calculated characteristic strength of the large cells.

This factor n would, however, change the determined characteristic area associated with the tests for the free foils. Since this area also enters the calculations for the high temperature strength, the same value for the characteristic strength for the large cells at high temperatures would be obtained. Hence, the results are insensitive to the absolute values used in Eq. (3), whereas the dependency of the stress on the deflection/thickness ratio in Eq. (3) is clearly verified by the similarity of the Weibull moduli for the free and glued electrolyte foils.

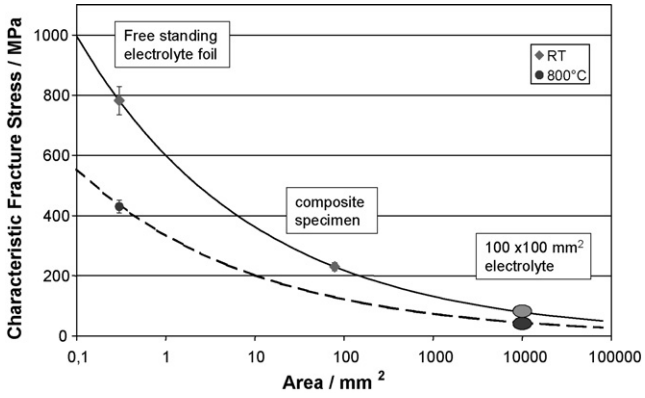

Fig. 6. Characteristic fracture stresses as a function of the stressed surface area. Free standing foil and cell data derived from results of composite specimens using Eq. (8).

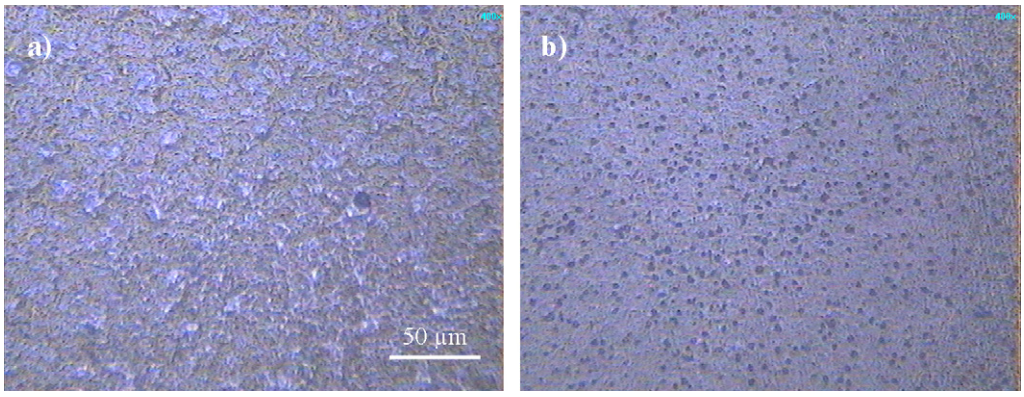

Fig. 7. Typical surface morphologies of the 3YSZ electrolyte foils. (a) Slightly rougher surface in and in b smoother surface.

5.2. 3YSZ electrolyte foils

The 3YSZ electrolyte foils had surfaces with only small variations in roughness, in contrast to the large roughness variations of the 6ScSZ foils (Fig. 7). Nevertheless, in order to test the surface effect specimens with either the slightly rougher or the slightly smoother surface under tension, tests were carried out RT. The general shape of the load–deflection curves was similar to that of the 6ScSZ foils. The average deflection at specimen failure was ~3.6 times the sheet thickness.

Using the approximation in Eq. (3) and the Weibull statistics of Eq. (7), values of $\sigma_0 = 1360 \pm 60$ MPa and $m = 7 \pm 3$ were obtained for the slightly smoother surface and $\sigma_0 = 1240 \pm 50$ MPa and $m = 8 \pm 3$ for the slightly rougher surface. Based on the similarity of the values for the different surface morphologies, a statistical analysis has been performed for all RT data yielding $\sigma_0 = 1300 \pm 40$ MPa and $m = 8 \pm 2$. Although the values agree within the limits of uncertainty, the slightly rougher surface of the 3YSZ foils was loaded under tension in the high temperature ring-on-ring experiments.

The load deflection curves for free-standing 3YSZ foils at 800 °C showed a similar shape, but failure occurred at a lower deflection (~2.5 times the thickness). The experimental data can be evaluated using the approximation in Eq. (3). The resulting characteristic fracture stress is $\sigma_0 = 610 \pm 20$ MPa with a Weibull modulus of $m = 10 \pm 4$. The Weibull modulus agrees within the limits of uncertainty with the value obtained at RT. The characteristic fracture stress is by a factor of ~2.1 lower than that at RT, which is similar to the factor of 1.8 obtained for the 6ScSZ electrolyte foils.

Applying the composite specimen approach, a characteristic fracture stress of $\sigma_0 = 600 \pm 30$ MPa ($m = 6 \pm 3$) was determined. Taking the results of all specimens into account as described explicitly for the 6ScSZ sheets, a single Weibull modulus of $m = 8.7 \pm 2.0$ is obtained. Based on this average Weibull modulus the stressed surface area of the free-standing electrolyte foil is calculated from Eq. (8) as ~0.1 mm^2, which agrees within the limits of uncertainty with the value for the 6ScSZ foils.

Again the data permit a prediction of the fracture stress of larger electrolyte sheets used as cells in a SOFC stack. The characteristic strength of a 10 cm × 10 cm cell of the 3YSZ electrolyte material is estimated to be 350 ± 115 and 170 ± 55 MPa at RT and 800 °C, respectively. A further reduction of the maximum applicable stress on 3YSZ electrolytes needs to be taken into account for lower failure probability. If the failure of only one cell in 1000 is permitted, stress limits of 160^{+84}_{-77} and 75^{+40}_{-36} MPa at RT and 800 °C, respectively should not be exceeded.

5.3. Comparison 6ScSZ and 3YSZ electrolyte foils

The fracture stress results of the two electrolyte materials showed a sensitivity to the roughness and morphology of the foil surfaces. The 6ScSZ electrolyte foils revealed a pronounced difference related to the surface roughness, whereas such an effect was not been observed for the 3YSZ electrolyte foils. A comparison of all results is given in Table 1, where for the 6ScSZ foils the values for the weaker surface are shown. Average Weibull moduli of $m = 5.3$ for the 6ScSZ electrolytes and $m = 8.7$ for the 3YSZ electrolytes are obtained. The higher Weibull modulus of the 3YSZ foils is an indication of a smaller spread in the defect size distribution. The higher m-value has especially a favorable effect on the fracture stresses for lower failure probabilities.

Table 1
Comparison of the fracture stresses for 6ScSZ ($m = 5.3 \pm 1.0$) and 3YSZ ($m = 8.7 \pm 2.0$) electrolyte foils

Characteristic fracture stress (MPa)	Free foil, RT	Free foil, 800 °C	Glued foil, RT	10 cm × 10 cm cell, calculated, RT	10^{-3} failure, 10 cm × 10 cm cell, RT	10 cm × 10 cm cell, calculated, 800 °C	10^{-3} failure, 10 cm × 10 cm cell, 800 °C
6ScSZ	780 ± 40	430 ± 21	230 ± 14	90 ± 40	25^{+20}_{-14}	50 ± 20	14^{+11}_{-8}
3YSZ	1300 ± 40	610 ± 20	600 ± 30	350 ± 115	160^{+84}_{-77}	170 ± 55	75^{+40}_{-36}
Ratio 3YSZ/6ScSZ	1.7	1.4	3.4	3.9	6.4	3.4	5.4

Considering the large surface area of SOFC cells (e.g. 100 mm × 100 mm) in a SOFC stacks, characteristic strengths of ∼90 MPa for RT and ∼50 MPa for 800 °C are estimated for the 6ScSZ electrolytes and ∼350 MPa for RT and ∼170 MPa for 800 °C for 3YSZ electrolyte. The values of the 3YSZ foil are a factor of ∼3.9 and ∼3.4 larger than that of the 6ScSZ foils. The decreases in strength at high temperatures of ∼44% for the 6ScSZ and 51% for the 3YSZ foils are similar to the decreases of ∼61% and ∼33% that have been reported for 3YSZ and 8YSZ electrolyte foils.[18]

Assuming a failure probability of 10^{-3}, the maximum stress that a 6ScSZ electrolyte foil of this cell size can withstand is only ∼25 MPa at RT and ∼14 MPa at 800 °C. For 3YSZ electrolyte foils of the same size the limits are factors of 6.4 and 5.4 higher especially due to higher Weibull modulus with ∼160 MPa for RT and ∼75 MPa for 800 °C.

6. Conclusions

The characteristic fracture stress and Weibull modulus have been determined for specimens from thin 6ScSZ and 3YSZ electrolyte sheets. Using the testing approach with composite specimens (foils glued on metallic substrate), it was possible to elucidate how the characteristic fracture stress depends on the stressed surface area and temperature.

Characteristic fracture stresses have been obtained for the 6ScSZ and 3YSZ electrolyte foils for RT and 800 °C and could be associated with the stressed surface areas. Predictions have been made for large surface area of SOFC cells (e.g. 100 mm × 100 mm) in a SOFC stacks and consideration has been given to the effect of the failure probability. Especially at lower failure probabilities and for larger cells, the tested 3YSZ foil material appears to be mechanically superior to the 6ScSZ electrolyte foils. The derived stress limits corresponding to tolerable failure probabilities should be considered in SOFC stack design.

Acknowledgements

The financial support of the German Federal Ministry of Economics and Technology (BMWi) is gratefully acknowledged (Contract no. 0327703A).

References

1. Napporn, T. W., Bedard, X. J., Morin, F. and Meunier, M., Operating conditions of a single-chamber SOFC. *J. Electrochem. Soc.*, 2004, **151**, A2088–A2094.
2. Malzbender, J., Steinbrech, R. W. and Singheiser, L., Failure probability of solid oxide fuel cells. *Ceram. Eng. Sci. Proc.*, 2005, **26–4**, 293–297.
3. Fischer, W., Malzbender, J., Blass, G. and Steinbrech, R. W., Residual stresses in planar solid oxide fuel cells. *J. Power Sources*, 2005, **73**, 150–153.
4. Malzbender, J., Wakui, T. and Steinbrech, R. W., Deflection of planar solid oxide fuel cells during sealing and cooling of stacks. In *Proceedings of the sixth Euro. SOFC Forum, vol 1*, 2004, pp. 329–338.
5. Malzbender, J., Wessel, E., Steinbrech, R. W. and Singheiser, L., Reduction and re-oxidation of anodes for solid oxide fuel cells. *Solid State Ionics*, 2005, **176**, 2201–2203.
6. Stöver, D., Buchkremer, H. -P. and Tietz, F., *VDI-Berichte Nr.,* 2002, **1680**, 209–266.
7. Malzbender, J., Steinbrech, R. W. and Singheiser, L., Determination of the interfacial fracture energies of cathodes and glass/ceramic sealants in a planar solid oxide fuel cell design. *J. Mater. Res.*, 2003, **18**, 929–934.
8. Malzbender, J., Steinbrech, R. W. and Singheiser, L., Strength of planar cells for SOFC application. In *Proceedings of the SOFC VIII*, 2003, pp. 1463–1472.
9. An, K., Halverson, H. G., Reifsnider, K. L., Case, S. W. and McCord, M. H., Comparison of methodologies for determination of fracture strength of 8 mol% yttria-stabilized zirconia electrolyte materials. *J. Fuel Cell Sci. Technol.*, 2005, **5**, 99–103.
10. Malzbender, J. and Steinbrech, R. W., Mechanical properties of coated materials and multi-layered composites determined using bending methods. *Surf. Coat. Technol.*, 2004, **176**, 165–172.
11. Schmitt, R. W., Blank, K. and Schönbrunn, G., Experimentelle Spannungsanalyse zum Doppelringverfahren. *Sprechsaal*, 1983, **116**, 397–405.
12. Kao, R., Perrone, N. and Capps, W., Large deflection solution of the coaxial-ring-circular-glass-plate flexure problem. *J. Am. Ceram. Soc.*, 1971, **54**, 566–571.
13. Deutsche Norm, "Bestimmung der Biegefestigkeit von Glas", DIN 1288-1, 2000.
14. Selcuk, A. and Atkinson, A., Strength and toughness of tape-cast yttria-stabilized zirconia. *J. Am. Ceram. Soc.*, 2000, **83**, 2029–2035.
15. Stolten, D., Monreal, E. and Seeselberg, C. testing of membranes via biaxial strength and proof testing device regarding nonlinear structural behaviour, in ceramics: charting the future, In Techna Srl, ed. P. Vincenzini. 1995, pp. 2613–2620.
16. Malzbender, J., Comment on hardness definitions. *J. Eur. Ceram. Soc.*, 2003, **23**, 1355–1359.
17. Morrel, R. "biaxial flexure strength testing of ceramic materials", NPL Report, Measurement Good Practice Guide No. 12, 1998.
18. Atkinson, A. and Selçuk, A., Mechanical behaviour of ceramic oxygen ion-conducting membranes. *Solid State Ionics*, 2000, **134**, 59–66.